ULTRASTRUCTURE OF BACTERIZED AND AXENIC TROPHOZOITES OF *ENTAMOEBA HISTOLYTICA* WITH PARTICULAR REFERENCE TO HELICAL BODIES

ROBERT M. ROSENBAUM and MURRAY WITTNER

From the Department of Pathology, Albert Einstein College of Medicine, New York 10461

ABSTRACT

Electron microscopy of bacterized and axenic trophozoites of *Entamoeba histolytica* showed only slight differences in ultrastructure between the two. As with other species of *Entamoeba* so far studied, this species lacks typical mitochondrial structures and formed endoplasmic reticulum. Dense clusters of glycogen particles are especially characteristic in axenic amebas. Microtubular structures 360 A in diameter appear randomly oriented in both bacterized and axenic trophozoites. Ribonucleoprotein (RNP) bodies are of two typical forms—elongate, parallel arrays of helices (the classical chromatoid bodies), and short helical fragments. Both kinds of helix show a recurring pitch angle of 68–80° and an over-all diameter of 480 A. RNP particles comprising the helices average 180 A in diameter. The longitudinal axes of adjacent helices are 440 A apart. Following RNase digestion of water-soluble methacrylate sections, helices show a core approximately 60 A in diameter. Short helices are also associated with digestive vacuoles. Free RNP particles per se are never seen within digestive vacuoles, but intact short helices are frequently detected closely associated with the external membrane of digestive vacuoles. In some cases, continuation of externally intact helical forms could be related to filamentous material within the vacuole. Acid phosphomonoesterase activity could be demonstrated within digestive vacuoles where deposition of reaction product is especially intense on the filamentous material.

The successful axenic cultivation of *Entamoeba histolytica* (13, 33) provides an important step toward further understanding of the nature of the host-parasite-bacterial interrelationship, inasmuch as data derived from axenic cultures can be interpreted more reliably in terms of the ameba itself without bacterial interference. Furthermore, preparation of material for electron microscopic, as well as cytochemical studies, becomes simpler once bacterial associates are eliminated. Thus far, only *E. invadens* from the snake (6, 12, 29, 36) has been studied from axenic culture with the electron microscope (30).

It is desirable to know whether any ultrastructural changes take place when amebas are removed from normal association with host tissue and placed into bacterized culture, and especially into axenic culture. Alteration in nutrition is known to affect the basic structure of many kinds of cells in culture, as well as their means of acquiring and dealing with nutritional materials.

While the present study was initially designed to investigate the extent and nature of possible ultrastructural differences between trophozoites grown with or without bacterial associates, it soon became evident that little information was available concerning the functional significance of the organelles possessed by these amebas.

This is especially true of the chromatoid bodies so characteristic of the species of *Entamoeba* studied thus far.

Usually associated with cysts, chromatoid bodies were described in trophozoites by Geiman and Ratcliffe (15) in *E. invadens* and by Hopkins and Warner in *E. histolytica* (20). Subsequent studies (18) suggested that the chromatoid bodies were not serving simply as storage material in the cyst, which would then be consumed during the trophozoite stage. Indeed, Barker and Deutsch (5) demonstrated that, in *E. invadens*, the bodies increased in size with age in the trophozoite and decreased with age in cysts. These observations were confirmed by electron microscopy (12) demonstrating also that components of the chromatoid body were crystalline masses of RNA, of approximately 200–300 A dimension, which either became disaggregated or reaggregated to form the typical chromatoid body as described with the light microscope. The appearance of *Entamoeba invadens* crystalline material as helical subunits (29, 30) is suggestive of polysomes (23, 28), although such functional significance cannot yet be assigned to them with certainty. In the present paper, the possible association of the chromatoid or ribonucleoprotein (RNP) bodies with other intracellular organelles in the trophozoites of axenic *E. histolytica* are described, and observations relative to possible functional significance are presented.

MATERIAL AND METHODS

Materials

BACTERIZED CULTURES: Bacterized cultures originally derived from a K-9 strain of *E. histolytica* were employed for these studies. These cultures were isolated from an experimentally-produced guinea pig liver abscess, and maintained in this laboratory for over 2 yr in Cleveland and Collier's medium (Bacto Entamoeba Medium, No. 0053-01, Difco Laboratories, Inc., Detroit, Mich.). Cultures were maintained at 36°C, and were transferred three times weekly.

AXENIC CULTURES: Strains F-22 and 301 (*E. histolytica*) were maintained at 36°C in the medium described by Wittner (33). The cultures were considered to be in optimal growth every 3–4 days and were transferred weekly.

Methods

COLLECTION AND FIXATION OF AMEBA: For initial harvesting of amebas, the entire culture tube was centrifuged for 5 min (room temperature) at 1000 rpm, and 1–2 ml of medium from the bottom of the slant was pipetted into 13 ml of cold 2% glutaraldehyde-phosphate buffer (pH 7.2). This "wash" treatment, lasting for a total of 5 min, was accomplished during centrifugation in the cold at 1000 rpm for the entire interval. It appears to be critical for optimal preservation of cells without undue precipitation of protein from the culture phase onto the surface of the ameba. The supernatant was carefully removed to the last 1–1.5 ml, and fresh buffered 2% glutaraldehyde was added. Fixation continued in the cold for 30 min. The tube was again centrifuged in the cold at 1000 rpm, the supernatant was removed, and the ameba were resuspended in cold phosphate buffer (pH 7.2) for 5 min followed by centrifugation in the cold for 3 min. After removal of the supernatant, cold 1% osmium tetroxide-phosphate buffer (pH 7.2) was added for 20 min and additional centrifugation (10 min) was carried out at 3000 rpm to form a loose pellet. The osmium tetroxide was removed, and more phosphate buffer was added carefully so as not to disturb the pellet. The pellet was left in cold phosphate buffer for at least 1 hr, after which it was dehydrated in ethanol and propylene oxide and embedded in Araldite.

ELECTRON MICROSCOPY: Sections were cut with a diamond knife on an LKB Ultrotome and placed on carbon- or carbon-Formvar-coated grids. They were routinely stained in 0.5% lead (Reynolds) alone for 10 min or with a combination of lead (2 min) preceded by 0.5% aqueous uranyl acetate (10 min).

Electron micrographs were taken with an RCA EMU3F operating at both 50 and 100 kv.

DNA/RNA DIGESTION: We employed the method described by Leduc and Bernhard (21), using water miscible glycol methacrylate with Luperco as a catalyst. Amebas were fixed in 2% phosphate-buffered glutaraldehyde. Methacrylate polymerization proceeded for 3 days. Commercial RNase and DNase[1] were dissolved in phosphate buffer at pH 6.5–6.8 in concentrations of 0.1%. Incubation at 37°C proceeded for various times up to 4 hr by floating sections on the surface of the enzyme solution, washing with double distilled water, staining, and final transfer to grids.

LOCALIZATION OF ACID PHOSPHOMONOESTERASE ACTIVITY: Trophozoites were collected by short, rapid centrifugation, followed by a fixation wash of cold 2% glutaraldehyde in 0.1 M cacodylate buffer at pH 7.2. After a second centrifugation, the supernatant was discarded and the precipitate was

[1] DNase, electrophoretically purified from beef pancreas, RNase-free; RNase, from bovine pancreas, protease-free (Sigma Chemical Co., St. Louis, Mo.)

washed in cold fixative-buffer. Fixation proceeded in the same medium in the cold for 60 min. After several washes with distilled water, the precipitate was incubated in Gomori's (Microscopic Histochemistry. 1952. University of Chicago Press, Chicago. 952) medium with glycerophosphate as substrate at pH 5.6, either at room temperature (60 min) or at 37°C (20–30 min). After incubation, the precipitate was washed in distilled water and postosmicated in 1% osmium tetroxide-phosphate buffer (pH 7.2). Dehydration and embedding for electron microscopy proceeded as described above. Controls consisted of omitting glycerophosphate from the incubation medium.

OBSERVATIONS

General Appearance of Bacterized and Axenic Trophozoites

Trophozoites grown in association with bacteria are active feeders and showed numbers of vacuoles containing bacteria in various stages of digestion (Fig. 1). Other vacuoles contained membranous structures, in part derived from digested bacteria. Amebas from axenic cultures (Fig. 2) generally showed smaller vacuoles that never contained the amount of debris detected in bacterized animals. Axenic trophozoites also appeared to possess more RNP crystalline bodies than did cells from bacterized cultures. The distinguishing features of a typical trophozoite of *E. histolytica* are summarized in Fig. 12.

NUCLEUS: No differences could be detected between nuclei of bacterized and axenically-grown trophozoites. Although the nucleus appears spherical most frequently (Fig. 1), it may also appear irregular in outline (Figs. 2, 3). It is bounded by a double membrane broken frequently and with regularity by nuclear pores (Fig. 3). These pores show a well-developed electron-opaque system about 700–800 A across. There is no fibrous laminar lining such as has been described in the closely related axenically-grown *E. invadens* (30).

Chromatin at the periphery of the nucleus appears as discontinuous aggregate masses with varying degrees of electron opacity (Figs. 1, 3). Both axenic and bacterized trophozoites possess vesicular structures restricted to the chromatin region (Figs. 1, 3). These are bounded by a double membrane and range in diameter from 0.16 to 0.2 μ as shown by serial sections. Such structures do not appear to be invaginations of the cytoplasm into the plane of section of the nucleus and, therefore, they represent an intranuclear structure. They have been described in bacterized *E. histolytica* (22), as well as *E. invadens* (30).

The endosome is small, occupying approximately one-fifth of the nucleus, and consists of uniform electron-opaque masses (Fig. 3) approximately in the center of the nucleus.

CYTOPLASMIC VACUOLES: A clear-cut feature serving to distinguish between axenically-grown and bacterized trophozoites is the over-all difference in size of vacuoles present in individual cells and the nature of their contents. Trophozoites from bacterized cultures appeared to have fewer small vacuoles; the contents of the larger vacuoles consisted of bacteria in various stages of digestion and a variety of debris usually appearing as membranes (Figs. 1, 5), or membrane fragments. Vacuoles in cells from axenic culture frequently appeared empty, but occasionally contained some debris in the form of membrane fragments (Fig. 2).

In addition to large digestive vacuoles, both bacterized and axenic *E. histolytica* show a category of small, vacuole-like structures scattered in the cytoplasmic matrix (Figs. 4, 7). These appeared far more sensitive to fixation than the larger digestive vacuoles.

CYTOPLASMIC RESERVE MATERIALS: Although we could detect no lipid in material prepared for electron microscopy, oil red O staining of amebas regularly revealed small lipid droplets by ordinary light microscopy. Presumably lipid was lost during the embedding process for electron microscopy. Large carbohydrate reserves in the form of glycogen were present in both kinds of trophozoite. This glycogen appears to be of the α-configuration (26). Glycogen granules were always present within trophozoites, but it was impossible to distinguish patterns specifically marking axenic or bacterized cells (Figs. 1, 2). In any single group of either axenic or bacterized cells prepared for study, some amebas showed areas of accumulations of packed glycogen granules, the remaining areas of cytoplasm being relatively devoid of carbohydrate reserve material (Fig. 4). The significance of such "glycogen centers" is unknown.

OTHER ORGANELLES: No mitochondria or mitochondria-like structures could be detected in trophozoites of *E. histolytica* (Figs. 1, 2, 4).

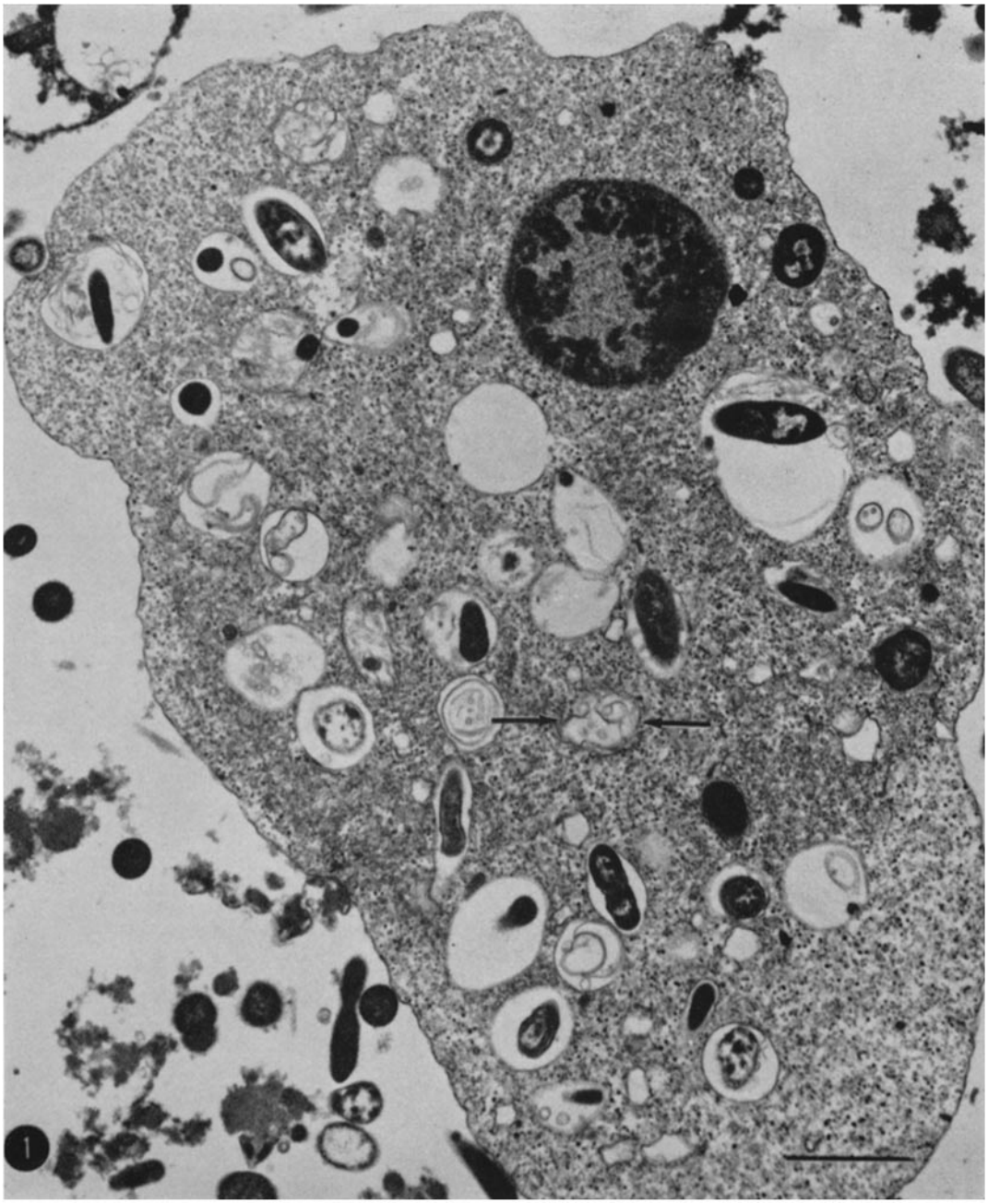

FIGURE 1 Bacterized trophozoite of *E. histolytica* fixed in glutaraldehyde followed by OsO_4. Vacuoles containing bacterial fragments and membranous debris can be seen. A single vacuole (arrows) shows evidence of autophagy. The granular appearance of the cytoplasm is chiefly due to glycogen, although numerous free, short helices are also present. No large chromatoid bodies are present in this section. The nucleus shows the characteristic internal vesiculation described in the text. Scale = 2.0 μ. × 8400.

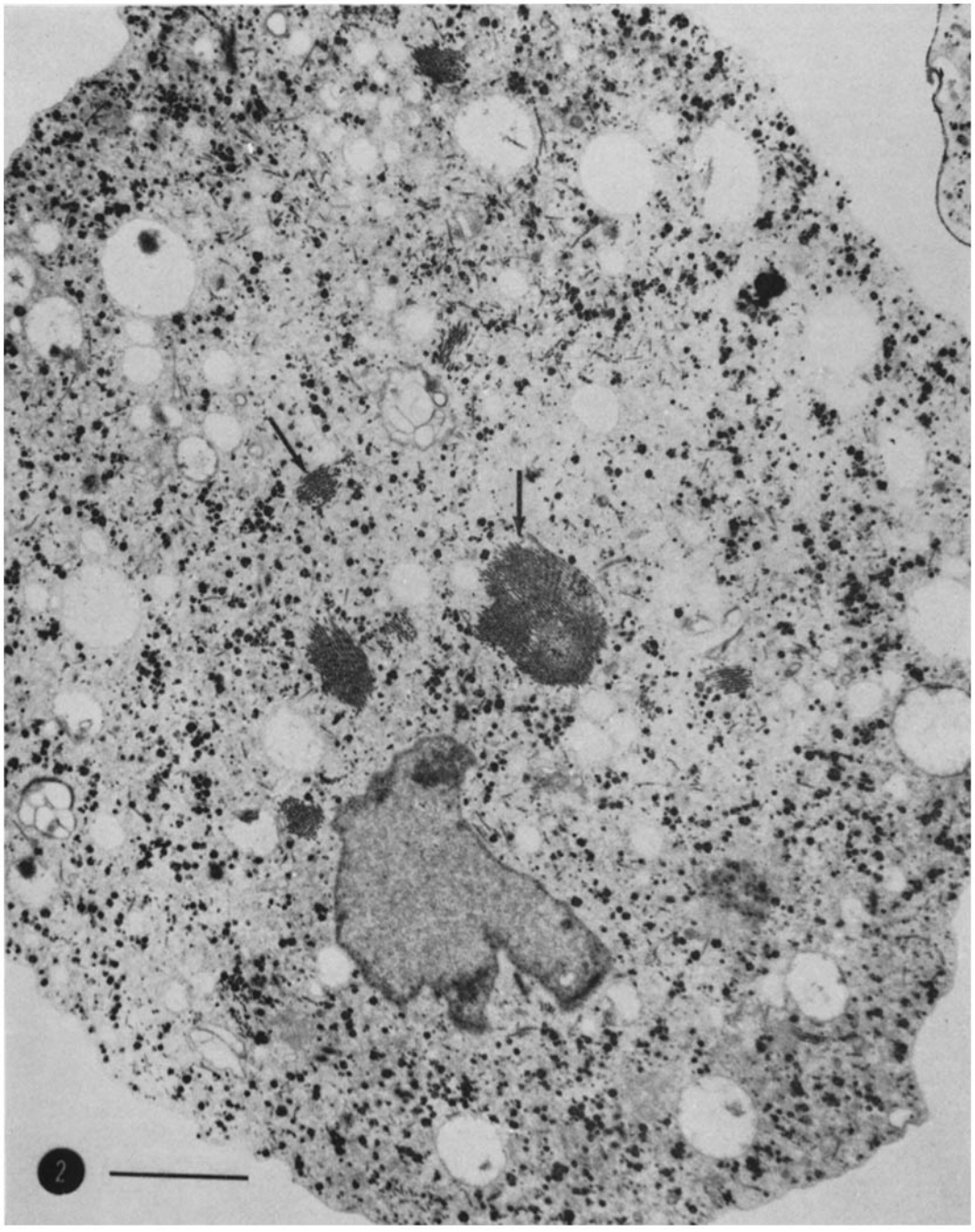

FIGURE 2 Axenic trophozoite of *E. histolytica* fixed as described in Fig. 1. Vacuoles are generally free of debris in contrast to those of bacterized amebas, although some vacuoles contain traces of membranous material. Less glycogen is present than in bacterized trophozoites, so that small clusters of glycogen can be detected readily in the cytoplasm. Several crystalline RNP helices are evident (arrows). Scale = 2.0 μ. × 8400.

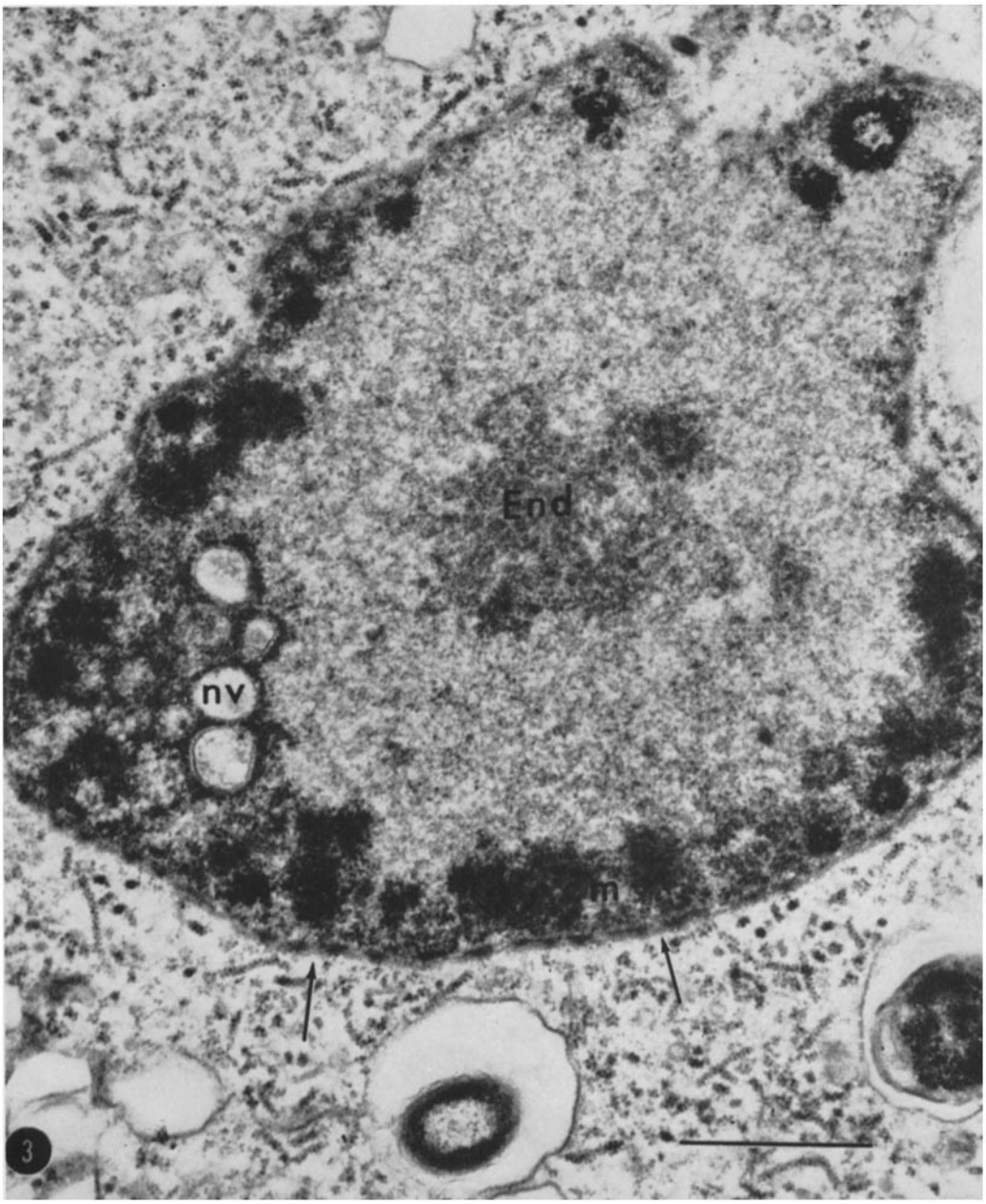

FIGURE 3 Nuclear ultrastructure in a bacterized trophozoite of *E. histolytica* fixed in glutaraldehyde, postosmicated, and stained with lead and uranyl. The endosome (*End*) and membrane-bounded nuclear vesicles (*nv*) are evident. The latter contain some electron-opaque material. A concentration of chromatin material (*cm*) appears at the nuclear margin. Pores (arrows) are visible in the nuclear envelope. Numerous small helical fragments are free in the cytoplasmic matrix. Scale = 1.0 μ. × 28,000.

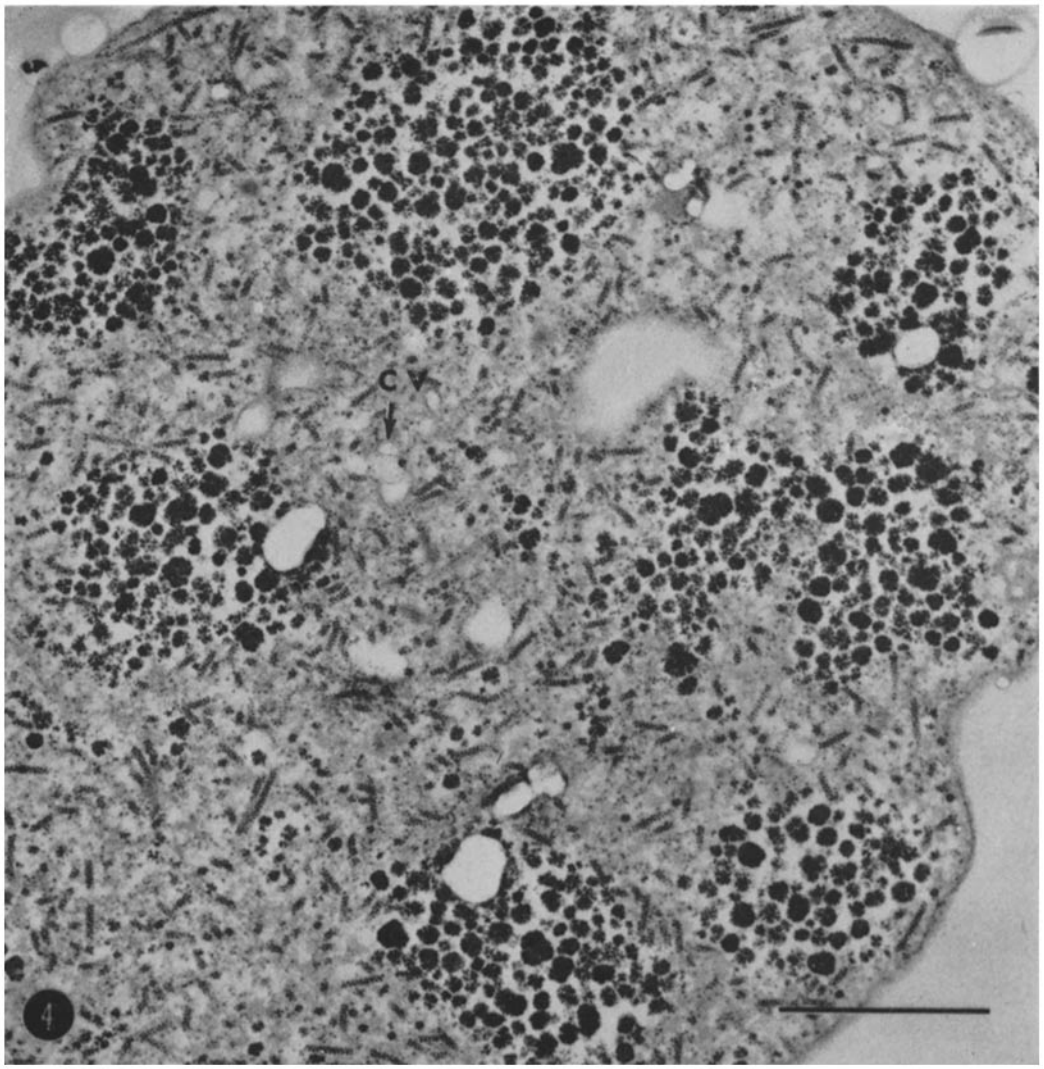

FIGURE 4 Axenic trophozoite showing glycogen centers scattered through the cytoplasmic matrix. Components of the cytoplasmic vacuolar system (*cv*) can be seen. Note the large numbers of short helices in the cytoplasm. Scale = 1.0 μ. × 28,000.

This observation is consistent with that found in other representatives of the genus *Entamoeba* (12, 22, 25, 30, 36), some trichomonads (1, 2), and some free-living amebas as well (3).

Microtubular structures were present in both kinds of trophozoites, and they appeared as packed, but randomly oriented, electron-opaque structures, approximately 360 A in diameter (Fig. 7). Although a microtubule of this size is larger than most of the intracellular microtubular elements reported thus far, dimensions of this magnitude have been described, usually in experimental conditions involving the breakdown of tubular protein (9). In our present material it was not possible to ascertain whether these large tubular structures represent degradative phenomena in the trophozoite.

RNP (CHROMATOID) BODIES: Characteristic of those several species of *Entamoeba* studied thus far (4–6, 29, 30), these structures form linearly arranged aggregates that are the typical crystalline chromatoid bodies seen under the light

microscope (15, 18, 20). Studies by Barker (4, 6) have emphasized their largely ribonucleoprotein nature in *E. invadens*.

Both packed and fragmented or dispersed RNP bodies were present in the cytoplasm of axenic and bacterized trophozoites of *E. histolytica*. Longitudinal sections of RNP aggregates appeared as electron-opaque bodies stacked up to 20 deep. They were of varying length depending on their orientation at the time of sectioning. Although they appeared to show rigidity, they were not rigidly attached throughout their length and both aggregates and single helices appeared flexible (Figs. 2, 4, 5). The aggregates lie at random in the cytoplasm, and frequently as many as 15 or more such "crystalline" bodies of varying size appeared in a section of a single cell.

The crystalline structures may be interpreted as stacked helices when cut parallel to their long axes. Single helices showed a recurring pitch angle of between 68 and 80° when the method described by Weiss and Grover (32) was used. The helical cross-sectional diameter was approximately 480 A. Within a single helix (Fig. 8) a tetrad configuration can be found frequently on cross-section although pentads and hexads are also found (Fig. 5). Clearly, the tilt of the sectioned helix can determine the final configuration. On the basis of our measurements, the particles associated with the helix are 160–200 A (average = 180 A) in diameter and, therefore, correspond, as might be expected, with other cytoplasmic ribosomes. The longitudinal axes of adjacent helices in the packed arrays are approximately 440 A apart.

Following incubation at 37°C for 4 hr in RNase, an electron-opaque, filamentous core could be visualized (Fig. 6 B). Each filament appeared approximately 60 A in diameter, although the incubation procedure in combination with the water-soluble embedding medium that we employed did not provide any degree of fine resolution (Figs. 6 A, B). Although precise comparison between Araldite sections of these stacked arrays and water-soluble methacrylate sections must be viewed with caution, the amount of separation between the filament bundle axes in Araldite sections was 440 A, similar to that in water-soluble embedding media. Filament bundles from digested sections appear held together by an amorphous, electron-opaque material (Fig. 6 B).

Fragments, identical in all other respects to the units making up the stacked helical RNP arrays, were scattered at random throughout the cytoplasm (Figs. 4, 5, 8). Our measurements indicate that these helices correspond to portions of the stacked crystalline arrays. The fragments were most numerous in bacterized trophozoites or in axenic trophozoites fed bacteria in which they appeared oriented especially about digestive vacuoles. Such RNP fragments may be derived from the larger RNP aggregates from which they could break off, or assemblies of small helices could form the larger crystals (Fig. 12). In their association with vacuolar membranes, identifiable, electron-opaque RNP bodies making up the helical arrangement of the complex do not pass into the vacuole (Figs. 5, 7, 8). At the inner side of the vacuolar membrane, however, single or double filaments approximately 60 A in cross-section, presumably derived from central core material of the RNP helical fragment, could often be detected (Fig. 5).

SURFACE PHENOMENA: We made numerous observations on regions near the surface of axenic trophozoites, bacterized trophozoites, and axenic trophozoites fed bacteria. In many cases it was possible to observe changes at the surface when bacteria were found in close proximity to trophozoites. Fig. 9 illustrates the relationships between the short helical fragments, the plasmalemma, and the immediately adjacent cytoplasmic area. Typically, an apparent breakdown of the plasmalemma takes place accompanied by the formation of a surface bleb. Numerous short helices appear in this region and several of them seem to organize perpendicular to the cell surface. Ribosome particles forming the helix do not appear in the bleb, but electron-opaque material, possibly core material, can be seen in the cytoplasmic discharge (Fig. 9, single arrows). In the immediately surrounding extracellular area, double filaments, approximately 60 A in diameter, similar to those described in digestive vacuoles (Fig. 5, for example), were seen frequently.

LOCALIZATION OF ACID PHOSPHATASE ACTIVITY: Acid phosphatase activity was restricted to the walls of digestive vacuoles and their contents (Figs. 10, 11). Control sections showed no deposition of reaction product. In axenic trophozoites we could visualize association of reaction product with vacuolar contents clearly not bacterial in origin. Reaction product was often associated with filamentous material that ex-

FIGURE 5 Relationships between a food vacuole and short helices in a bacterized trophozoite of *E. histolytica*. Several helices are oriented toward and touch on the vacuolar membrane at points (single arrows). At these sites, where the helix approaches the membrane, a loss of ribosomal material leaves an electron-opaque "filament" within the vacuole. These filaments are evident extending from the inner membrane side. Some filaments appear double and appear to also represent core material (double arrows). Scale = 0.5 μ. × 72,000.

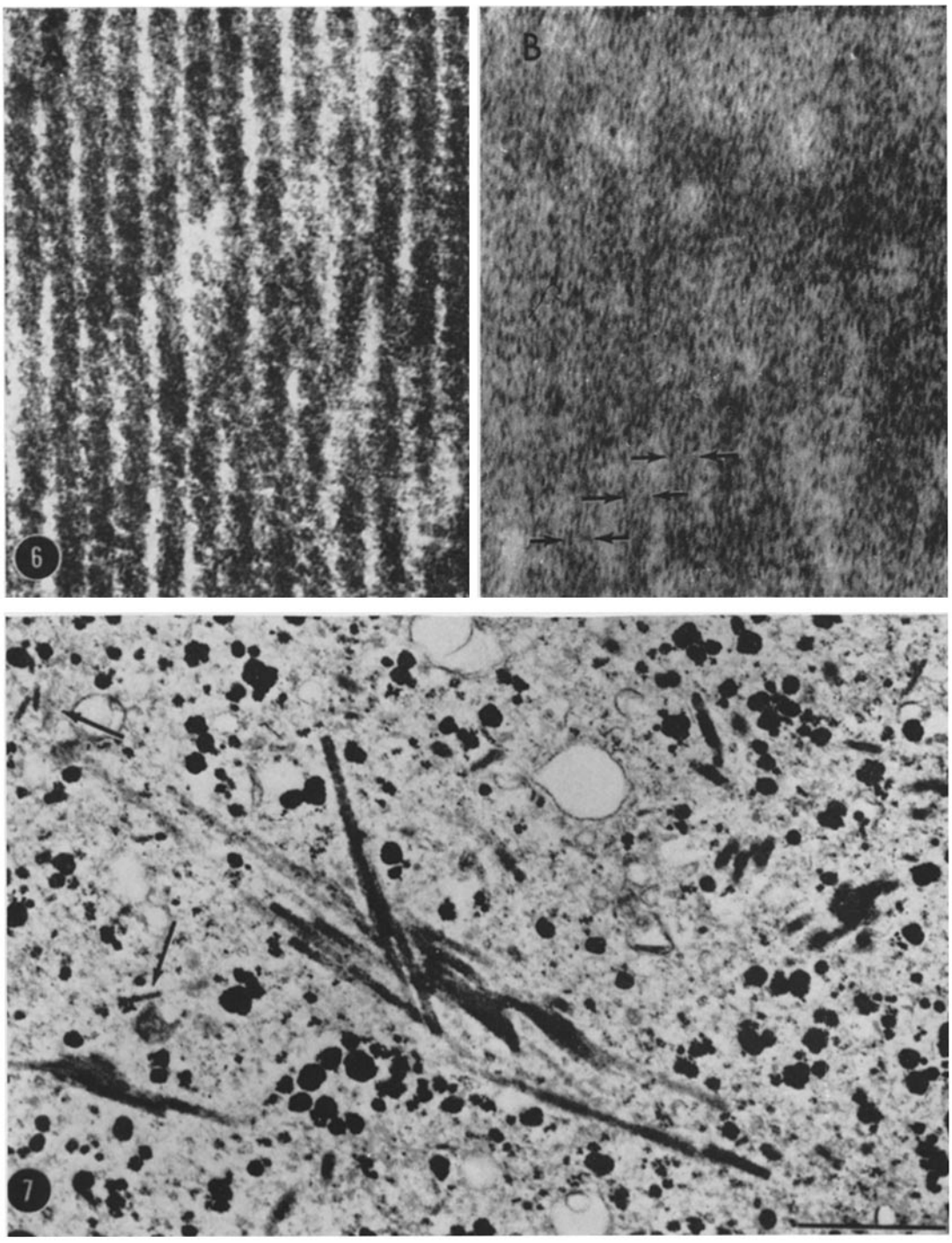

FIGURE 6 A and B Both electronmicrographs represent an area from a packed helix of a glutaraldehyde-fixed, postosmicated axenic trophozoite of *E. histolytica*. Cells were embedded in water-soluble methacrylate, sections mounted on grids were exposed to buffered (pH 6.7) ribonuclease for up to 4 hr at 37°C. The digestion procedure and properties of the embedding medium have reduced resolution. × 115,000. (A) Control section incubated in buffer at pH 7.4 (37°C for 4 hr). RNA helices with an approximate distance of 440 A between their axes are evident. (B) Section of packed helix incubated in RNase at 37°C for 4 hr. Ghosts of individual helices are evident between the pairs of horizontal arrows. Distance between arrows is approximately 440 A. Filaments with an approximate 60 A thickness are within the remnants of each helix.

FIGURE 7 Microtubular aggregates within the cytoplasm of an axenic trophozoite of *E. histolytica*. Such tubules stain heavily with uranyl acetate and are randomly distributed, usually in clusters. They may be compared in size to several small helical fragments seen in this figure (arrows). Scale = 1.0 μ. × 24,000.

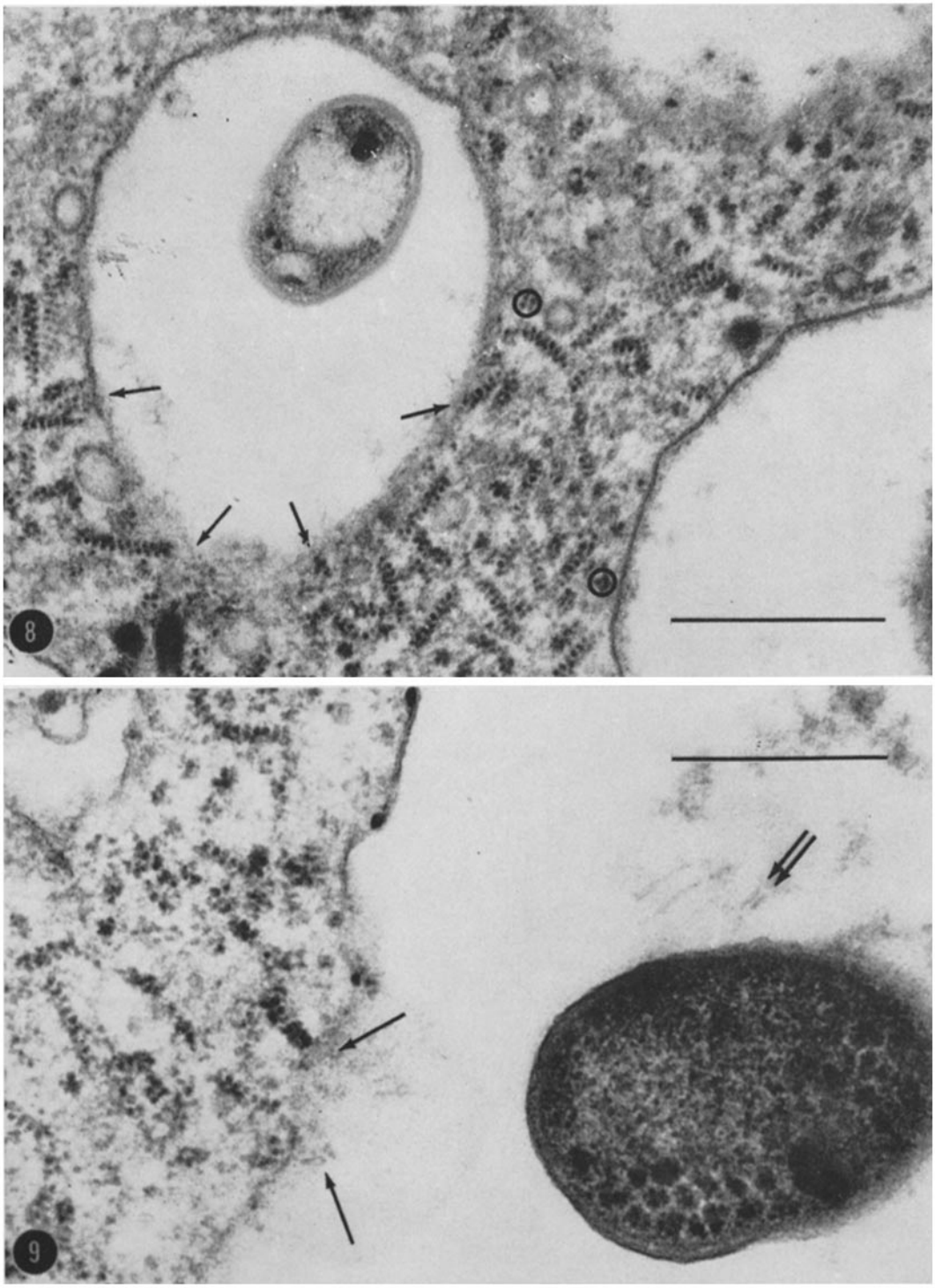

FIGURE 8 Relationships between a digestive vacuole and short RNP helices in a bacterized, but originally axenic, trophozoite of *E. histolytica*. Numerous small RNP helical fragments are closely associated externally with the vacuolar membrane (arrows). At points of contact, electron-opaque core material can be seen on the inner side of the vacuolar membrane. A cross-section of a helical fragment with typical tetrad conformation is seen within the circle. Scale = 0.5 μ. × 72,000.

FIGURE 9 Surface of an axenic trophozite of *E. histolytica* exposed (15 min) to a culture of *E. coli* and sectioned serially. The electronmicrograph shows local breakdown of the plasmalemma with formation of a cytoplasmic bleb. Several short helices (out of several that have accumulated perpendicular to the surface) appear to release material within the bleb itself. Electron-opaque material clearly related to the helices is evident distal to the bleb area (single arrows). Some filaments with a double configuration (double arrows) appear extracellularly. Scale = 0.5 μ. × 72,000.

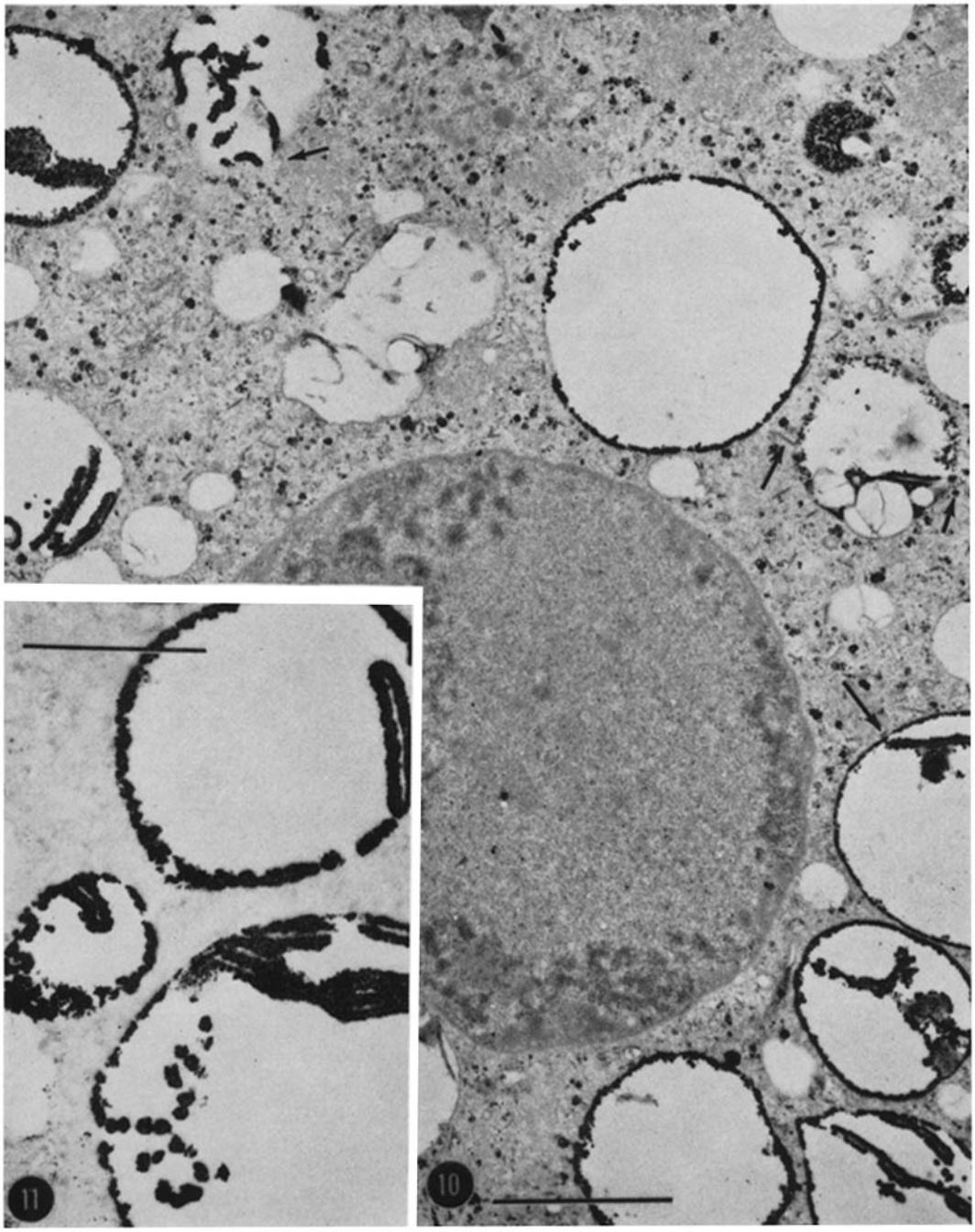

FIGURE 10 Axenic trophozoite of *E. histolytica* stained for acid phosphatase activity with glycerophosphate at pH 5.6 as substrate. Most digestive vacuoles show deposition of reaction product about the inner surface of the vacuolar membrane. Debris within vacuoles shows reaction product. Numerous filaments, some extending from the inner surface of the vacuolar membrane, show reaction for acid phosphatase activity. At several sites (arrows), short helical bodies can be detected in the cytoplasmic matrix that appear associated with these stained filaments. The nucleus and the cytoplasmic matrix show no false-positive reaction product. Scale = 2.0 μ. × 12,500.

FIGURE 11 Three digestive vacuoles from an axenic trophozoite stained for acid phosphatase activity. Reaction product appears about the inner aspect of the vacuolar membrane. At several sites, reaction product is associated with filaments extending from the inner membrane. Scale = 1.0 μ. × 28,000.

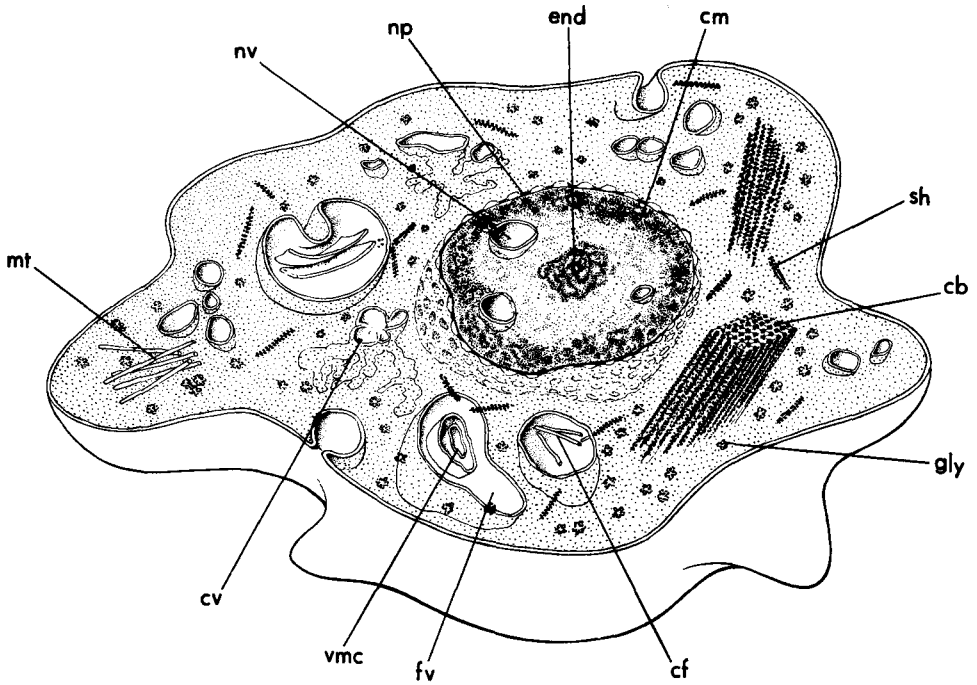

FIGURE 12 Composite drawing including described ultrastructural features of a typical trophozoite of *E. histolytica*. *cb*, crystalline body; *gly*, glycogen; *cf*, core filamentous material; *mt*, microtubules; *cm*, chromosomal material; *np*, nuclear pore; *cv*, cytoplasmic vacuolar system; *nv*, nuclear vesicle; *end*, endosome (nucleolar equivalent); *sh*, short helix; *fv*, food vacuole; *vmc*, vacuolar membrane contents.

tended frequently from the inner vacuolar wall toward the interior of the vacuole (Figs. 10, 11). Although it was difficult to determine precisely the diameter of such filaments in sections stained for acid phosphatase activity, due to variations in deposit of reaction product, the diameter appeared to be approximately 400–450 A. This range includes the 440 A spacing of the double filamentous core material derived from helical bodies seen on the inner aspect of the membranes of digestive vacuoles (Fig. 5).

Reaction product was also deposited along the inner surface of vacuolar membrane, although not all vacuoles showed activity (Fig. 10). Cellular debris within the lumen showed deposition of reaction product (Fig. 10), but rarely was the reaction diffuse within the vacuoles. Some material showed no evidence of being associated with enzymic activity.

No other sites in the cytoplasm of either axenic or bacterized trophozoites showed evidence of acid phosphatase activity.

DISCUSSION

The present study reemphasizes many ultrastructural similarities between *E. histolytica* (14, 22, 25) and the several other *Entamoeba* species that have thus far been investigated by electron microscopy. Among these may be included lack of classically formed mitochondria, Golgi structures, lysosomal equivalents, and the presence of helical ribonucleoprotein bodies and their subfragments. Structural features, such as the nuclear nets described for *E. invadens* (30) and many other protozoa (7, 17), are not present in *E. histolytica*.

Practically no difference in ultrastructure could be detected between axenic and bacterized trophozoites by the methods we used. Increased numbers of helical subfragments, presumably derived from the larger helical RNP bodies, appeared to be present in amebas grown in continuously bacterized culture, or in axenic amebas exposed to bacteria. More quantitative data on this observation, however, are needed.

The presence of crystalline bodies composed largely of ordered arrays of ribosomal material

is of particular interest, since species of *Entamoeba* studied thus far do not possess a membranous endoplasmic reticulum containing ribosomal particles (4–6, 12, 15, 22, 25, 29, 30, 36). Therefore, the helical structures appear to represent the sole sites of organized ribosome location in these organisms. As with *E. invadens*, the RNP helices in trophozoites of *E. histolytica* present two aspects—densely packed linear arrays and subunits scattered at random in the cytoplasmic matrix. Both packed arrays and the subfragments in *E. histolytica* show dimensional interrelationships similar to those described by Morgan and Uzman (24) for *E. invadens* on the basis of optical Fourier analyses. Essentially, the geometric configurations of both kinds of protozoan helices appear identical to, and possess many of the properties of, polyribosomal configurations from other cell types including differentiating cells (8–10, 16, 23, 31), as well as HeLa cells (28). Weiss and Grover (32) and Behnke (8) have reported pitch angles from crystalline bodies that are apparently closely related to those in *Entamoeba*. Our results, with the use of RNase digestion of water-soluble methacrylate sections of *E. histolytica*, are the first to suggest a filamentous substructure in polyribosome-like material of this kind, although the presence of core material has been suggested (24, 32). Barker and Deutsch (5) first calculated the cross-sectional diameter of the packed ribosomal helical arrays to be 200 A, but they could not detect internal organization. Morgan and Uzman (24), calculating the diameters for individual spherical ribosomal units, obtained an "empty" core value of 60 A, although the possibility that real core material was present was suggested. Weiss and Grover (32) refer to cylindrical ribosomal carrier columns of constant dimension in HeLa cells, but consider these to represent polyribosomal units.

Our observations show that, while short RNP helices approach digestive vacuoles and even appear to attempt penetration, helical fragments themselves could not be detected within vacuoles. We could, however, detect the presence of single and double filaments within vacuoles and they may represent the filamentous core from previously intact helices, suggesting that vacuolar penetration of helical core material may occur as the helix becomes denuded of RNP particles. Alternatively, the filamentous structures could represent a discharge of helical material, perhaps of core origin, into digestive vacuoles. Similar structures were observed surrounding bacteria about to be phagocytized by amebas. These observations, as well as a preliminary study of the enzymic activity of digestive vacuoles and the ribosomal helices closely associated with them (34, 35), suggest that the small helices may be related to increased levels of hydrolase activity present during digestion, and that filaments may contain, or actually represent, enzymic protein. This premise agrees with the observation that the number of short helices increases about digestive vacuoles and at the cell surface when axenic trophozoites are fed bacteria (34). In addition, evidence that filaments within digestive vacuoles show acid phosphomonoesterase activity is very provocative, and suggests their role in the supply, if not the production, of at least some kinds of enzyme protein.

On the basis of the present observations, we can only speculate as to the relationship between short helices, the large crystalline bodies and digestive vacuoles. The absence in *E. histolytica* of most of the usual cytoplasmic organelles and the presence of highly organized and apparently dynamic RNP material in helical form suggest the possibility that these structures may have a multifaceted and extremely labile role in the economy of the ameba. The observations showing intimate association of the short helices with both food and autophagic vacuoles, and the demonstration of acid phosphomonoesterase activity on what appears to be helical core material within digestive vacuoles suggest that enzymic protein synthesis may be occurring in association with the larger RNP bodies themselves, and that newly synthesized protein may be carried via the short helices to digestive vacuoles. If such could be demonstrated, then, in that they show association with acid phosphomonoesterase activity, the ribosomal helices in *Entamoeba* may be regarded as functioning as a type of primary lysosome synthesizing enzyme protein on demand (35). Whether, in *E. histolytica*, they are similarly identifiable with the other kinds of enzymic activity shown biochemically (11, 27) as well as histochemically (19) remains to be determined.

This study was supported by grants (AI 07371, GM 05483, and AM 03605) from the United States

Public Health Service, and Contract DA-49-193-MD-2932 from the United States Army Medical Research and Development Command, Armed Forces Epidemiological Board. Dr. Wittner is a Career Scientist of the Health Research Council of the City of New York.

Received for publication 22 September 1969, and in revised form 15 December 1969.

BIBLIOGRAPHY

1. ANDERSON, J. 1955. The electron microscopy of *Trichomonas muris*. *J. Protozool.* **2**:114.
2. ANDERSON, E., and H. W. BEAMS. 1959. The cytology of *Tritrichomonas* as revealed by the electron microscope. *J. Morphol.* **140**:205.
3. ANDERSON, N., C. CHAPMAN-ANDRESEN, and J. R. NILSSON. 1968. The fine structure of *Pelomyxa palustris*. *C. R. Trav. Lab. Carlsberg.* **36**:285.
4. BARKER, D. C. 1963. A ribonucleoprotein inclusion body in *Entamoeba invadens*. *Z. Zellforsch. Mikrosk. Anat.* **58**:641.
5. BARKER, D. C., and K. DEUTSCH. 1958. The chromatoid body of *Entamoeba invadens*. *Exp. Cell Res.* **15**:604.
6. BARKER, D. C., and V. SVIHLA. 1964. Localization of cytoplasmic nucleic acid during growth and encystment of *Entamoeba invadens*. *J. Cell Biol.* **20**:389.
7. BEAMS, H. W., T. N. TAHMISIAN, R. L. DEVINE, and E. ANDERSON. 1959. The fine structure of nuclear envelope of *Entamoeba blattae*. *Exp. Cell Res.* **18**:366.
8. BEHNKE, O. 1963. Helical arrangement of ribosomes in the cytoplasm of differentiating cells of the small intestine of the rat foetus. *Exp. Cell Res.* **30**:597.
9. BENSCH, K. G., R. MARANTZ, H. WISNIEWSKI, and M. SHELANSKI. 1969. Induction *in vitro* of microtubular crystals by *Vinca* alkaloids. *Science (Washington).* **165**:495.
10. BYERS, B. 1967. Structure and formation of ribosome crystals in hypothermic chick embryo cells. *J. Mol. Biol.* **26**:155.
11. DANFORTH, W. F. 1967. Respiratory metabolism. *In* Research in Protozoology. T. Chen, editor. Pergamon Press Ltd., Oxford. **1**:205.
12. DEUTSCH, K., and V. ZAMAN. 1959. An electron microscope study of *Entamoeba invadens* Rodhain. *Exp. Cell Res.* **17**:310.
13. DIAMOND, L. 1961. Axenic cultivation of *Entamoeba histolytica*. *Science (Washington).* **134**:336.
14. FLETCHER, K. A., B. G. MAEGRAITH, and R. JARUMILINTA. 1962. Electron microscope study of trophozoites of *Entamoeba histolytica*. *Ann. Trop. Med. Parasitol.* **56**:496.
15. GEIMAN, Z. M., and H. L. RATCLIFFE. 1936. Morphology and life cycle of an amoeba producing amoebiasis in reptiles. *Parasitology.* **28**:208.
16. GHIARA, G., and C. TADDEI. 1966. Dati citologici e ultrastrutturali su di un particolare tipo di constituenti basofili del citoplasma di cellule follicolari e di ovociti ovarisi di rettili. *Boll. Soc. Ital. Biol. Sper.* **42**:784.
17. GRASSÉ, P. P., and J. THEODORIDES. 1957. L'ultrastructure de la membrane nucléaire des gregarines. *C. R. Acad. Sci. (Paris).* **245**:1985.
18. HAKANSSON, E. G. 1936. Observations in the chromatoid bodies in cysts of *E. histolytica*. *U.S. Naval Med. Bull.* **24**:478.
19. HELLER, A., and H. REDLICH, 1969. Enzymmuster der *Entamoeba histolytica*. *Progr. Protozool. Proc. 3rd Int. Congr. Protozool. (Abstracts), Leningrad.* 263.
20. HOPKINS, D. L., and K. L. WARNER. 1914. Functional cytology of *Entamoeba histolytica*. *J. Parasitol.* **8**:133.
21. LEDUC, E. H., and W. BERNHARD. 1967. Recent modifications of the glycol methacrylate embedding procedure. *J. Ultrastruct. Res.* **19**:196.
22. MILLER, J. H., J. C. SWARTZWELDER, and J. E. DEAS. 1961. An electron microscope study of *Entamoeba histolytica*. *J. Parasitol.* **47**:577.
23. MONNERON, A. 1969. Experimental induction of helical polysomes in adult rat liver. *Lab. Invest.* **20**:178.
24. MORGAN, R. S., and B. G. UZMAN. 1966. Nature of the packing of ribosomes within chromatoid bodies. *Science (Washington).* **152**:214.
25. OSADA, M. 1959. Electron microscopic studies of protozoa. I. Fine structure of *Entamoeba histolytica*. *Keio J. Med.* **8**:99.
26. REVEL, J. P. 1963. Electron microscopy of glycogen. *J. Histochem. Cytochem.* **12**:104.
27. SEAMAN, G. R. 1953. Inhibition of succinic dehydrogenase of parasitic protozoans by an arseno- and phospho-analog of succinic acid. *Exp. Parasitol.* **2**:366.
28. SCHARFF, M., and E. ROBBINS. 1966. Polyribosome disaggregation during metaphase. *Science (Washington).* **151**:992.
29. SIDDIQUI, W. A., and M. A. RUDZINSKA. 1963. A helical structure in ribonucleoprotein bodies of *Entamoeba invadens*. *Nature (London).* **200**:74.
30. SIDDIQUI, W. A., and M. A. RUDZINSKA. 1965. The fine structure of axenically-grown trophozoites of *Entamoeba invadens* with special refer-

ence to the nucleus and helical ribonucleoprotein bodies. *J. Protozool.* **12**:448.

31. WADDINGTON, C. H., and M. M. PERRY. 1963. Helical arrangement of ribosomes in differentiating muscle cells. *Exp. Cell Res.* **30**:599.
32. WEISS, P., and N. B. GROVER. 1968. Helical array of polyribosomes. *Proc. Nat. Acad. Sci. U.S.A.* **59**:763.
33. WITTNER, M. 1968. Growth characteristics of axenic strains of *Entamoeba histolytica*, Schaudinn, 1903. *J. Protozool.* **15**:403.
34. WITTNER, M., and R. M. ROSENBAUM. 1968. Control of virulence and invasibility in *Entamoeba histolytica. Bull. N.Y. Acad. Med.* **44**:1152.
35. WITTNER, M., and R. M. ROSENBAUM. 1969. The control of biosynthetic mechanisms in *Entamoeba. Progr. Protozool. Proc. 3rd Int. Congr. Protozool. Leningrad.* 19.
36. ZAMAN, V. 1961. An electron microscope observation of the 'tail' end of *Entamoeba invadens. Trans. Roy. Soc. Trop. Med. Hyg.* **55**:263.